Microbial pathogens and strategies for combating them: science, technology and education

Vol. 1

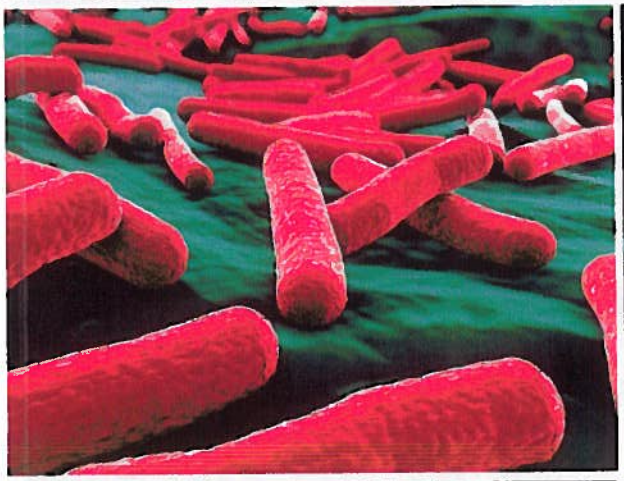
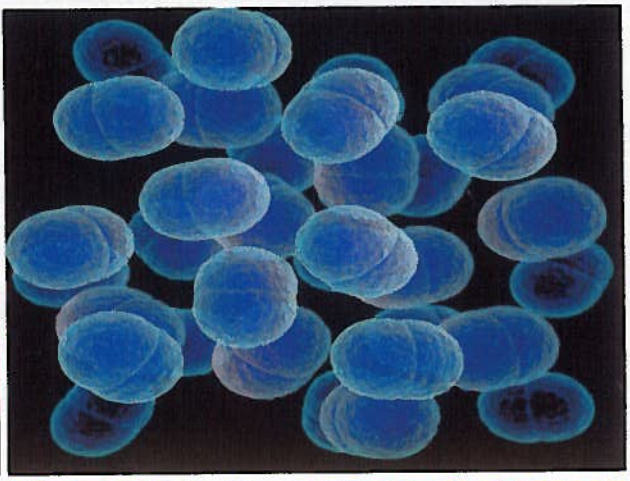
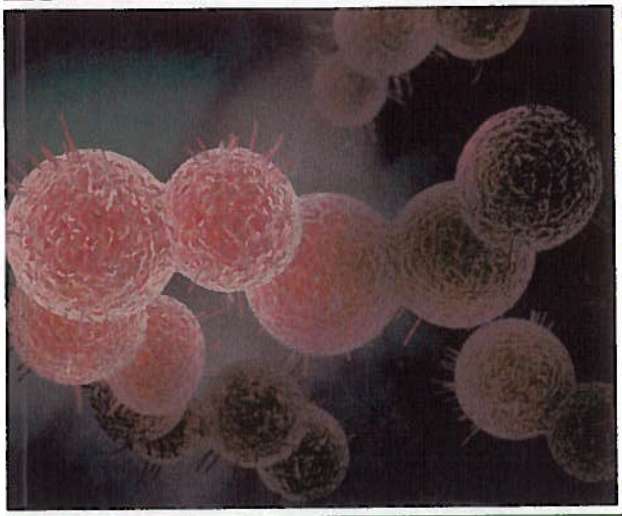


A. Méndez-Vilas (Ed.)

FORMATEX

Microbiology Book Series #4

Inhibition of siderophore biosynthesis by targeting *A. fumigatus* ornithine hydroxylase: A structure-based virtual screening study

S. Badieyan[1] and P. Sobrado[1,2,*]

[1]Department of Biochemistry, Virginia Tech, Blacksburg, VA 24061, USA
[2]Virginia Tech Center for Drug Discovery, Virginia Tech, Blacksburg, VA 24061, USA

Siderophore A (SidA) from *Aspergillus fumigatus* is a flavin-dependent monooxygenase that catalyses the hydroxylation of L-ornithine. N^5-hydroxyl-ornithine is subsequently incorporated into hydroxamate-containing siderophores. The pathogenicity of *A. fumigatus* in mammals is dependent on the availability and function of siderophores. Thus, inhibition of the siderophore biosynthetic pathway may significantly affect the virulence of this fungus. SidA plays a central role in this pathway and is considered the key target for inhibitory study. Availability of several high-quality structures of SidA in complex with different ligands allowed the *in-silico* screening of a large library of drugs, natural products, and synthetic compounds. The screening results were sorted by the absolute and normalized binding energies and then filtered based on the formation of at least one hydrogen bond to the part of the ornithine binding site with several hydrogen bond donors. The top hits have average molecular weights of 200 Da and free energy of binding of -7.5 kcal/mol. The compounds are highly soluble nitrogen- or oxygen-rich and make several hydrogen bonds with residues in the active site of SidA.

Keywords *Aspergillus fumigatus*, ornithine hydroxylase (SidA), inhibitor, flavin-dependent monooxygenase, virtual screening, docking experiments, anti-fungal drugs.

1. Introduction

1.1. *N*-ornithine hydroxylases as targets for treating fungal infections

rophore A (SidA) is an *N*-hydroxylating flavin-containing monooxygenase (NMO) that catalyzes the formation of ydroxyornithine (Scheme 1) in the biosynthesis of hydroxamate-containing siderophores in bacteria and fungi [1. iderophores are low molecular weight iron chelators [3, 4] produced by invading pathogens to scavenge iron from mammalian host during infection [5, 6]. Hydroxamate-containing siderophores in some fungal species, such as *rgillus fumigatus*, have been shown to be essential for pathogenesis [7, 8]. *A. fumigatus* is responsible for about of invasive aspergillosis, mainly in immune-compromised individuals [9]. The activity of SidA has been shown to sential for pathogenesis of *A. fumigatus*, validating this enzyme as a potential drug target [10-12].

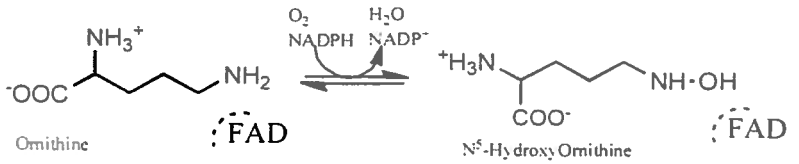

Scheme 1 General reaction catalyzed by SidA.

1.2. Structure and mechanism of SidA

rystal structures of SidA in complex with several ligands including ornithine, lysine, and arginine in the oxidized educed state and in the presence or absence of $NADP^+$ were recently solved by x-ray crystallography [13]. The codes of each structure along with related details are listed in Table 1. The structure of SidA is predicted to be a etramer with three main domains including an FAD-binding domain, $NADP^+$-binding domain, and a ligand- ng domain (Fig. 1A). Three main conformational changes in the structure of SidA can be observed upon the tion of FAD by NADPH, including an approximate 180° turn in the amide group of nicotinamide that allows the nated N5 of the isoalloxazine ring to make a hydrogen bond with the carbonyl group (O) of nicotinamide (Table addition, Arg144, which is expected to be involved in the binding of NADPH, and Met101, which is in van der s distance of the isoalloxazine, move away from the binding region of FAD and $NADP^+$ [13]. The rest of the n remains almost unchanged upon reduction; even after substrate binding there are no significant conformational es observed and the RMSD values calculated for the Cα do not exceed 0.3 Å for all conformations [13].

Table 1 Structural details of SidA conformations in complex with different ligands and at different redox states. The active site water molecules interacting with ligands in each complex are also indicated.

PBD Code	Resolution (Å)	Redox State	State of NADP	Ligand	N5(FAD)/Nictinamide orientation	Waters in main active site
4B63	1.9	Oxidized	$NADP^+$	Orn	N5 (FAD)...N (NADP)	32/41/42/28
4B64	2.28	Oxidized	$NADP^+$	Lys	N5 (FAD)...N (NADP)	42
4B65	2.32	Reduced	NADP(H)	NA	N5 (FAD)...O (NADP)	Not available
4B66	2.9	Reduced	NADP(H)	Arg	N5 (FAD)...O (NADP)	48
4B67	2.75	Re-Oxidized	$NADP^+$	Orn	N5 (FAD)...O (NADP)	Not available
4B68	2.29	Re-Oxidized	$NADP^+$	Arg	N5 (FAD)...O (NADP)	28/41
4B69	2.3	Oxidized	NA	Orn	NA	Not available

1.3. Amino acid binding domain of SidA

SidA is selective for L-ornithine but is also able to hydroxylate L-lysine with an 8-fold lower rate relative to ornithine. L-Arginine enhances the formation of a C4a-hydroperoxyflavin intermediate but is not a substrate for hydroxylation [14-16]. These three ligands have the same binding site in the main cavity of SidA [13]. In Fig. 1B, ornithine is presented in the binding site where its main chain makes a salt bridge to Lys107 and hydrogen bonds to Ser469 and Asn293 and the amino group. Phe296 makes a hydrophobic interaction to the side chain of ornithine. The site of hydroxylation of ornithine (N5) is within hydrogen bonding distance to the hydroxyl groups of the 2'-hydroxyl of the ribose in the nicotinamide ring and Asn323. The structures containing ornithine, lysine, and arginine are superimposed in Fig. 1C. All three ligands are attached in their expanded conformations. The binding site residues show no significant structural adjustment in response to the binding of different ligands but co-crystalized water molecules present in the active site vary in each complex (maybe due to the weak electron density). In Fig. 1C, the water molecules that are in hydrogen bonding distance of any ligand are illustrated and are listed in Table 1 as well. Most of the water molecules in the binding site mediate the formation of a hydrogen bond between the ligand main chains and the protein. One of the water molecules of interest is the one observed in the oxidized SidA with ornithine (PDB:4B63) and in the re-oxidized state in complex with arginine (PDB:4B68). The water molecule has the same position as expected for the distal oxygen of the C4a-hydroperoxyflavin intermediate (water 28). In Fig. 1D, the proposed conformation of the intermediate is shown. A hydrogen bond between the carbonyl of $NADP^+$ and the N^5 of the reduced flavin and a hydrogen bond with the ribose sugar of $NADP^+$ stabilize the C4a-hydroperoxyflavin intermediate.

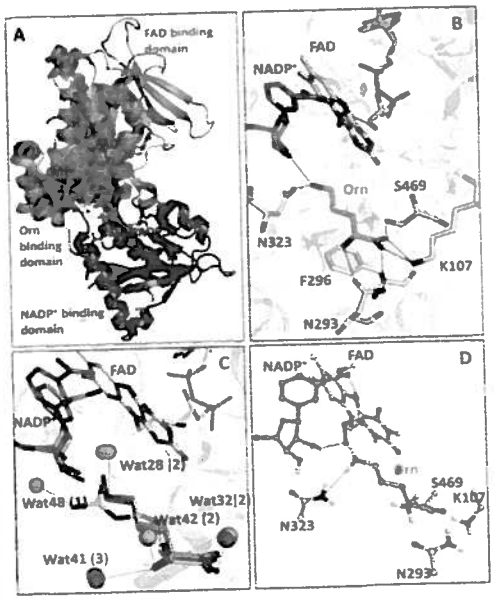

Fig. 1 A) The three main binding domains of SidA, including the FAD binding domain (cyan), NADP(H) binding domain (blue), and ornithine binding domain (pink). B) Ornithine binding domain in the active site of SidA (data taken from PDB 4B67). C) The position of water molecules in the active site of SidA. The available conformations of SidA-ligand complexes were structurally aligned and the water molecules available in different structures are colored with the same color of corresponding ligand (amino acid) of that structure. Arginine, lysine and ornithine are represented in green, pink and cyan respectively. The water molecules, which appear in the same position are named with a similar arbitrary number (as it is in Table 1). D) Proposed conformation of the C4a-hydroperoxyflavin intermediate of SidA. The hydrogen bonds made by the ligand (ornithine) and $NADP^+$ (hydroxyl group of ribose) stabilize the peroxide intermediate.

2. Methods

2.1. Docking/Screening procedures

All the docking and screening studies in this work were conducted using AutoDock-Vina [17] and protein structures and compounds were prepared by Auto-Dock tools 1.5.2 [18]. Three Vina replicates were conducted for each ligand in the cross-docking and re-docking steps, while a single run was performed for screening. For structural model testing, in addition to the original crystal structures, energy-minimized structures were also evaluated. Energy minimizations of liganded and unliganded structures were performed using united atom Gromos96 53GA6 force fields [19] incorporated in the Gromacs 4.5.5 software package [20]. Before simulations, the missing loops of SidA structures were built using ModLoop [21] based on *ab-initio* loop refinement in Modeller 9v7 [22] and the partial residues were completed using the rotamer library of PyMol [23]. The algorithm used by Vina for finding favorable positions of ligands in the active site of proteins does not count hydrogen atoms into its calculation; however, the protonation state of active site residues needs to be evaluated and assigned correctly before docking. H++ programs [24] were used to estimate pK_a values for ionizable amino acids and then polar hydrogens were added using pdb2gro tool of the Gromacs program. In addition, to access the impact of protein dynamics on ligand binding and screening, a set of short Molecular Dynamics (MD) simulations (5 ns) of unliganded SidA (PDB: 4B67) was conducted and twenty snapshots of MD trajectories based on RMSD clustering were taken to examine the effect of active site local changes on ligand binding. System preparation, minimization, equilibration, and MD production steps were setup as previously described [25].

As mentioned before, no significant conformational change is induced in the active site of SidA due to ligand binding, and ligands are able to bind in both oxidized and reduced states in the presence or absence of $NADP^+$ (Table 1). To evaluate the active site cavities, AutoLigand [26], as part of AutoDock tools [18], was used to search the binding site. A grid size of 16×16×14 Å was used to analyze the binding site and the entire entrance of the protein while a larger grid size of 20×18×18 Å was applied to calculate the cavity size including both ligand binding domain and $NADP^+$ binding domain (the part of domain for binding of nicotinamide-beta-riboside plus one phosphate group). The binding site cavity is marginally connected to the entrance cavity that lets molecules larger than ligands attach to SidA by expanding their interactions to both the binding site and the entrance cavity. In Fig. 2 the shape and the size of these internal cavities of SidA are illustrated.

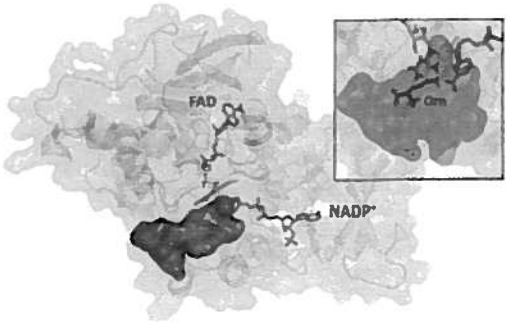

Fig. 2 Surface presentation of the binding site cavity and the entrance cavity in the SidA structure as calculated by AutoLigand. The cavities are colored in dark blue while the rest of the protein is illustrated in light blue. In the box, a side view of the cavity is presented and the ornithine molecule is shown as the reference.

2.2. Ligand library construction

All the libraries used for virtual screening include only compounds that follow Lipinski's rule of five (not more than 5 hydrogen bond donors or 10 hydrogen bond acceptors in their structures, their molecular mass less than 500 daltons, and logP less than 5) [27, 28]. These libraries were divided into three main categories: 1) Drug and Drug-like: including source catalog size of DrugBank (approved, experimental, nutritional) and CheMBL Drugstore and Collaborative Drug Discovery (filtered-out), a total of slightly more than 75,700 compounds. 2) Natural product: The compounds not included in the first category including natural derivatives and products provided by the compound libraries of Indofine, Nubbe, TimTec, and Ambinter with a total of over 68,342 compounds. 3) Synthetic library: a set of compounds that were selected based on structural properties such as solubility (solubility not less than 1 mM) and structural similarity to the current ligands of SidA. As this library does not include compounds from the two other categories it is considered a library of synthetic compounds and includes 322,550 small molecules. All the catalogs were taken from the ZINC database [29].

3. Results and Discussion

3.1. Docking analyses for re-docking and cross-docking

Re-docking and cross-docking of co-crystalized ligands is the first step to be examined to evaluate the reliability of the software for *in-silico* screening and determine the parameters needed to be setup such as charge distribution. Re-docking and cross-docking mainly help to identify and select one SidA structural model that would be appropriate for all screening studies. All seven SidA complexes were evaluated by this method (Table 2), including the binary structure (PDB: 4B69, no $NADP^+$ bonded) that has the ligand (ornithine) bound in the same position as it binds to the ternary conformation (with $NADP^+$, PDB:4B67).

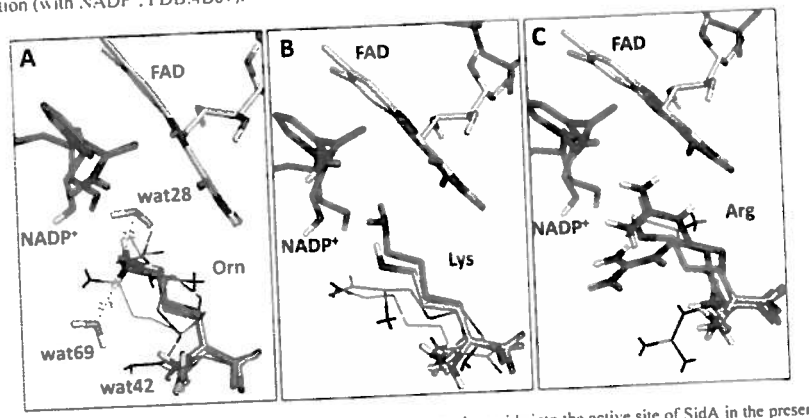

Fig. 3 Re-docking and cross-docking results from docking of different amino acids into the active site of SidA in the presence of co crystalized water 42 and/or "new water" 69. Ornithine in cyan is shown in all three figures as a reference (taken form PDB: 4B6 A) Presence of both wat69 and wat42 is required for correct re-docking of ornithine (ornithine in blue stick). Removal of any tw other water molecules led to the upside-down docking orientation of ornithine (presented in line format). B) For Lysine, although th presence of both water molecules gives decent cross-docking results (lysine in blue stick), the effect of wat69 is smaller and th presence of only wat42 may prevent the upside-down docking (Lysine in orange line illustratin). C) Presence and absence of wate gives two orientations of Arginine after cross-docking, in green and blue stick, respectively. Regarding the orientation of Arg PDB:4B66 or PDB:4B68, both oreinations can be accepted.

Almost all the re-dockings and cross-dockings in the absence of any water molecule failed to properly dock th ligands. The ligands bound in an upside down orientation in the binding site, with the amino and carboxylic group interacting with $NADP^+$ instead of with the side chain (Fig. 3 and Table 2). Adjustment of charge distribution in th active site for reduced or oxidized protein, taking neutral vs. positively charged ligand and/or energy minimization protein structures did not improve the re-docking RMSD. Among the structures, PDB:4B69 (with no bounded NADP shows lower values for RMSD although it was still large enough to seek other conditions which may impro orientation of the ligand in the active site of SidA. In the next step, all conformations were subjected to re-docking ar cross-docking with all the co-crystalized water molecules available in its binding site. A considerable improvement w observed but still not close to the ligand orientation in the crystal structure. Considering the position of water molecul in MD trajectories, we found that the addition of one water in the hydrogen bond distance of N5 of ornithine yiel perfect cross-docking and re-docking (Fig. 3A). This water molecule is named wat69 and in all MD simulations of Sic conformations a stable water molecule equivalent to wat69 can be observed. Elimination of other co-crystalized wa molecules one-by-one specified that co-crystalized wat42, beside wat69, is also required for perfect re-docking a cross-docking (Table 2). These two water molecule get less effective when increasing the size of the ligand. instance, arginine binds with an RMSD less than one in the absence of wat69. These data are consistence with docki studies performed using PvdA conformations (ornithine hydroxylase from *Pseudomonas aeruginosa* with 41% ident to SidA [30]). No water molecule is reported in submitted PvdA structure in complex to ornithine. Re-docking a cross-docking of ornithine only gave back the accurate positioning when the above two water molecules were added the equivalent positions in PvdA structures (data not shown).

Table 2 Values of RMSD (in Å) and free energy of binding (ΔG_b in Kcal/mol) for re-docking and cross-docking studies using available conformations of SidA. The values in red show re-dockings and the values in black are related to cross-dockings.

			PDB Code						
Ligand	Waters	Values	4B63	4B64	4B65	4B66	4B67	4B68	4B69
Orn	No-wat	RMSD	2.146	2.236	2.715	2.105	2.151	2.742	1.064
		ΔG_b	-4.9	-5.2	-5.3	-5.0	-5.1	-5.0	-4.7
	Wat-69-42	RMSD	2.112	0.884	1.437	2.081	2.112	2.133	0.876
		ΔG_b	-5.0	-5.4	-4.7	-5.3	-5.3	-5.1	-5.0
Lys	No-wat	RMSD	2.203	2.223	2.664	2.296	2.207	2.272	1.227
		ΔG_b	-5.4	-5.4	-5.4	-5.1	-5.4	-5.2	-5.0
	Wat-69-42	RMSD	1.003	1.002	1.303	0.778	2.240	0.731	0.848
		ΔG_b	-5.6	-5.7	-5.0	-5.8	-5.8	-5.4	-5.5
Arg	No-wat	RMSD	1.028	1.870	2.223	2.119	2.083	2.597	1.196
		ΔG_b	-6.4	-6.1	-6.3	-6.2	-6.4	-6.2	-6.0
	Wat-69-42	RMSD	1.136	1.157	2.347	1.255	2.314	2.171	1.145
		ΔG_b	-6.4	-6.6	-5.7	-6.4	-6.0	-6.1	-6.4

3.2. Analyses of virtual screening output

By analyzing docking and re-docking results, PDB:4B67 (with $NADP^+$ bound) and PDB:4B69 (no $NADP^+$ bound) were selected for conducting screening of large-scale libraries using Vina [25] on HokieOne and Athena supercomputer clusters at Virginia Tech. Vina output for each tested compound includes the free energy of binding sorted for different poses of that compound in the active site of SidA. Typically, the larger the compound the higher the binding energy. To avoid biased sorting, the most negative binding energy for each compound was normalized by dividing it by the number of heavy atoms of that molecule and the final sorting method was optimized based on both absolute and normalized energies. Lys107, Ser469, and Gln293, which make hydrogen bonds to the main chain of the ligands, are considered residues that make a region that consists of only hydrogen bond donors in the SidA active site. It is expected that a compound with a high free energy of binding will make at least one hydrogen bond in this region through its hydrogen bond acceptor groups. Thus, a restriction was applied to the screening output: the docked compounds should have at least one hydrogen bond donor (O, N, or F) in the hydrogen bond making distance (3.3 Å or less) to Lys107(N6) and Ser249(O).

As described above, the grid box defined for docking was large enough to encompass the main binding site, the entire enzyme entrance, and the nicotinamide-ribose binding domain (in case of PDB:4B69). Even though a large grid box was used, cross-docking and re-docking showed that the small ligands (Orn, Lys and Arg) only bound to the main binding site of SidA and not to the other cavities. However, the screening results included compounds that primarily bound to the entrance or the $NADP^+$ binding domains, therefore, other filtering criterion was applied to select the docked molecules that bind only to the main (ornithine) binding domain.

Table 3 The top hits of virtual screening of SidA against different libraries after sorting by binding energy and applying criteria. The binding energies with the prime symbol are the absolute free energy of binding and the other values refer to the normalized one. The binding energies in the presence and absence of water molecules are also compared.

				Binding energies (Kcal/mol)			
	ZINC #	Generic Name	Molecular structure	SidA/ NoWat	SidA/ Wat42	SidA/ Wat69-42	Solubility (mole/L)
Drug and Drug Like	ZINC09224016	Milrinone		-8.6', -0.54	-6.7', -0.48	-6.0', -0.43	3.20E-02
	ZINC06165883	Actarit	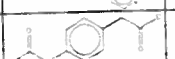	-7.4', -0.53	-6.6', -0.47	-6.2', -0.41	5.18E+00
	ZINC00897369	Nitrofural		-7.4', 0.53	-6.9', -0.49	-6.4', -0.46	2.80E-03
	ZINC00895199	Levodopa		-7.3', -0.52	-7.4', -0.53	-6.4', -0.46	1.40E-02
Natural Products	ZINC00901774	Willardiine		-7.0', -0.50	-7.1', 0.51	-4.6', -0.33	2.20E-02
	ZINC00403591	Securinine	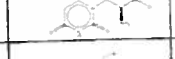	-7.6', -0.51	-6.5', -0.41	-5.4', -0.34	4.60E+00
	ZINC01843029	Allantoin		-6.3', -0.57	-6.6', -0.69	-7.0', -0.64	9.10E-02
	ZINC03860635	Mucic acid	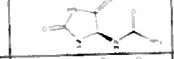	-6.3', -0.45	-6.4', -0.46	-6.7', -0.48	4.76E+00
Synthetic Compounds	ZINC01530298	L-ArgOH	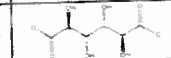	-7.0', -0.54	-6.9', -0.63	-6.6', 0.51	1.10E-01
	ZINC00967496	–	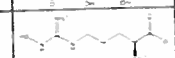	-8.2', -0.59	-8.6', -0.61	-8.9', -0.64	1.10E-03
	ZINC03662018	–	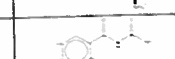	-7.9', -0.61	-8.1', -0.62	-8.3', -0.64	1.50E-03
	ZINC28629431	–	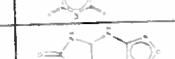	-7.4', -0.57	-7.7', -0.59	-8.0', -0.62	2.00E-01

Table 3 shows the selected top hits with their binding energies for each prepared library based on the above criteria. The theoretical solubility of each compound as calculated by Advanced Chemistry Development (ACD/Lab) shows that the final hits are considerably soluble (in the range of millimolar to molar). Predicted docked conformations for four compounds in Table 3 are exemplified in Fig. 4. These figures show that the selected top hits of virtual screening will follow the same hydrogen binding map in the active site of SidA as the ligands. The presence of Phe296 in the active site makes the staking hydrophobic interactions favorable; as a result, most of the docked molecules with large binding energy have an aromatic group or large alkyl chain (similar to Lys or Orn) as a main part of their structures. Interestingly, the top hits, mostly, have a nitrogen-containing group that is oriented the same as the amine group of Orn and Lys (N6) in the active site. The only issue with these results is the very small variation in the size of the selected final compounds. Since the docked compounds are filtered out based on binding to the main binding site of the protein and not the entrance cavity, the group of small molecules that only fill the cavity of the binding site were among the filtrates. To overcome this issue, considering the total number of hydrogen bonds made by the small molecules to the protein may help. These top hits have free energy of binding on average of -7.5 kcal mol ($K_i \approx 3$ μM), which is ~2.5 kcal/mol more stable relative to ornithine. If the direct output of screening is sorted based on the absolute binding energy, some large compounds (MW > 350 gr mol) with binding energies > -11.0 Kcal/mol will be observed among the top hits. However, analyses of solubility show these compounds, which usually consist of too many aromatic groups, are almost insoluble in biological buffers (solubility in range of μM or less).

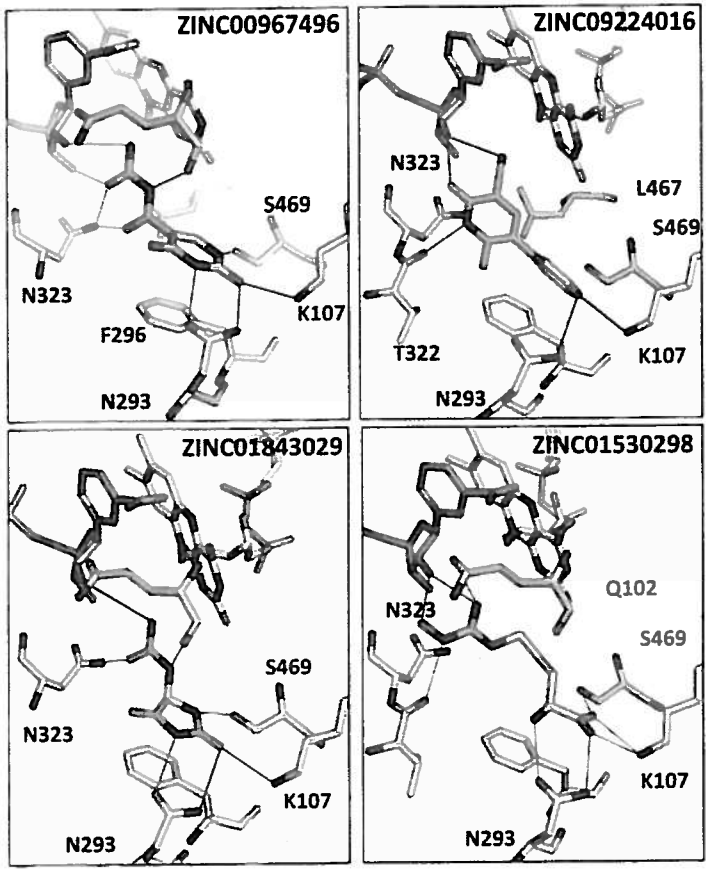

4 Examples of docked structures from the top hits of screening in the active site of SidA in the absence of any water (t ounds are highlighted in red in Table 3). The hydrogen bonds formed by the docked structures are illustrated in red (hydrogen length < 3.3 Å).

3.3. The role of water molecules in docking results

screenings were performed in the presence of both wat69 and wat42, only wat42, and with no water molecules in ctive site of SidA (Table 3). Since there is no reference structure, RMSD values for each compound in the presence absence of these water molecules cannot be calculated and compared; however, the free energies of binding for ed molecules when there is no water in the active site is usually higher relative to docking in the presence of water cules, indicating that the water molecules fill considerable space in the active site that does not allow the docked ounds to interact with atoms/residues. Visual analyses of molecules in the active site show for some compounds rientation of the molecule in the active site is extremely affected by the presence of water, while some other cules bind similarly under any condition. For instance, ZINC00967496, which is one of top hits from the synthetic y, positions itself in the active site so that it is trivially affected by water molecules (Fig. 5), while water induced ge reorientation in the docking position of ZINC09224016 (with the generic name Milrinone from the Drug y). The water molecules are required for perfect re-docking and cross-docking, but their role in the binding of compounds is not clear; thus, the safe margin in selecting the docked molecules from screening results is to look ose compounds that capture the same orientation in the presence and absence of water molecules.

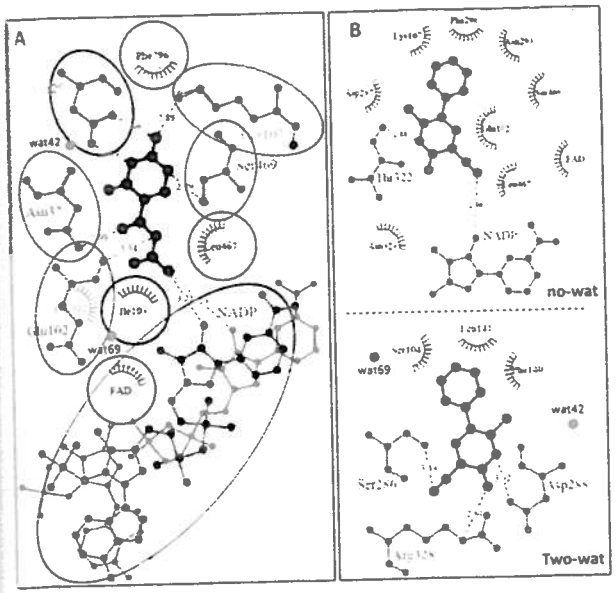

Fig. 5 Comparison the role of water molecules in the docking results. A) The presence of water molecules does not affect the orientation of the ZINC00967496 molecule in the active site. The main hydrogen bonds and hydrophobic interactions can be seen in both dockings. Figure shows the overlap of the LigPlot (Wallace *et al*, 1995) of ZINC00967496-SidA complex in the presence and absence of water molecules. B) In the presence of water molecules, ZINC09224016 prefers an orientation completely different from the one in the absence of water.

4. Conclusion

A. fumigatus virulence is dependent on the reaction catalyzed by SidA (hydroxylation of N^5-ornithine). Its role in pathogeneses, in addition to the fact that the active site of SidA is conserved in closely related invasive siderophore-dependent bacteria and fungi and not present in humans, make SidA a promising drug target. Currently, there are no reports of inhibitors with high affinity for SidA. In this study, the high resolution crystal structures of SidA were subjected to high throughput virtual screening against large libraries of drugs, natural products, and synthetic compounds. The raw results were filtered based on the positioning along the binding site and formation of hydrogen bonds to the conserved residues. The top selected hits are able to make several (at least three) stabilizing hydrogen bonds to active site residues and NADP. Based on absolute and normalized binding energy, visual analyses of binding in the active site, number of hydrogen bonds made by the molecule to the enzyme, and availability of biological studies or lacking of any report on toxicity, three compounds are finalized as the main candidates for inhibitory studies from the top hits of each library. Milrinone (ZINC09224016) [31], which is an inhibitor of phosphodiesterase and works as a medicine to increase the heart's contractility, Nitrofural (ZINC00897369) [32], a bactericidal compound, and ZINC00967496 [33], a synthetic compound can be considered as molecules with high potential for inhibition of SidA activity.

Acknowledgments This work was supported in part by grant from the National Science Foundation (MCB 1021384) and by the Virginia Tech Biodesign and Bioprocessing Center.

References

[1] Crosa JH, Walsh CT. Genetics and assembly line enzymology of siderophore biosynthesis in bacteria. *Microbiol Mol Biol Rev.* 2002; 66(2):223-249.
[2] Haas H, Eisendle M, Turgeon BG. Siderophores in fungal physiology and virulence. *Annu Rev Phytopathol.* 2008; 46:149-187.
[3] Neilands JB. Siderophores: structure and function of microbial iron transport compounds. *J Biol Chem.* 1995; 270(45):26723-26726.
[4] Hider RC, Kong X. Chemistry and biology of siderophores. *Nat Prod Rep.* 2010; 27(5):637-657.
[5] Weinberg ED. Iron availability and infection. *Biochim Biophys Acta.* 2009; 1790(7):600-605.
[6] Abergel RJ, Wilson MK, Arceneaux JEL, Hoette TM, Strong RK, Byers BR, Raymond KN. Anthrax pathogen evades the mammalian immune system through stealth siderophore production. *Proc Natl Acad Sci U S A.* 2006; 103(49):18499-18503.
[7] Lamont IL, Beare PA, Ochsner U, Vasil AI, Vasil ML. Siderophore-mediated signaling regulates virulence factor production in Pseudomonas aeruginosa. *Proc Natl Acad Sci U S A.* 2002; 99(10):7072-7077.

[8] Schrettl M, Bignell E, Kragl C, Joechl C, Rogers T, Arst HN, Jr., Haynes K, Haas H. Siderophore biosynthesis but not reductive iron assimilation is essential for Aspergillus fumigatus virulence. *J Exp Med*. 2004; 200(9):1213-1219.
[9] Tekaia F, Latge JP. Aspergillus fumigatus: saprophyte or pathogen? *Curr Opin Microbiol*. 2005; 8(4):385-392.
[10] Hissen AHT, Wan ANC, Warwas ML, Pinto LJ, Moore MM. The Aspergillus fumigatus siderophore biosynthetic gene sidA, encoding L-ornithine N-5-oxygenase, is required for virulence. *Infect Immun*. 2005; 73(9):5493-5503.
[11] Sokol PA, Darling P, Woods DE, Mahenthiralingam E, Kooi C. Role of ornibactin biosynthesis in the virulence of Burkholderia cepacia: Characterization of pvdA, the gene encoding L-ornithine N-5-oxygenase. *Infect Immun*. 1999; 67(9):4443-4455.
[12] Takase H, Nitanai H, Hoshino K, Otani T. Impact of siderophore production on Pseudomonas aeruginosa infections in immunosuppressed mice. *Infect Immun*. 2000; 68(4):1834-1839.
[13] Franceschini S, Fedkenheuer M, Vogelaar NJ, Robinson HH, Sobrado P, Mattevi A. Structural Insight into the Mechanism of Oxygen Activation and Substrate Selectivity of Flavin-Dependent N-Hydroxylating Monooxygenases. *Biochemistry*. 2012; 51(36):7043-7045.
[14] Chocklett SW, Sobrado P. Aspergillus fumigants SidA Is a Highly Specific Ornithine Hydroxylase with Bound Flavin Mononucleotide. *Biochemistry*. 2010; 49(31):6777-6783.
[15] Frederick RE, Mayfield JA, DuBois JL. Regulated O2 activation in flavin-dependent monooxygenases. *J Am Chem Soc*. 2011; 133(32):12338-12341.
[16] Romero E, Fedkenheuer M, Chocklett SW, Qi J, Oppenheimer M, Sobrado P. Dual role of NADP(H) in the reaction of a flavin-dependent N-hydroxylating monooxygenase. *Biochim Biophys Acta-Proteins Proteom*. 2012; 1824(6):850-857.
[17] Trott O, Olson AJ. AutoDock Vina: improving the speed and accuracy of docking with a new scoring function, efficient optimization, and multithreading. *J Comput Chem*. 2010; 31(2):455-461.
[18] Morris GM, Huey R, Lindstrom W, Sanner MF, Belew RK, Goodsell DS, Olson AJ. AutoDock4 and AutoDockTools4: Automated Docking with Selective Receptor Flexibility. *J Comput Chem*. 2009; 30(16):2785-2791.
[19] Oostenbrink C, Villa A, Mark AE, Van Gunsteren WF. A biomolecular force field based on the free enthalpy of hydration and solvation: The GROMOS force-field parameter sets 53A5 and 53A6. *J Comput Chem*. 2004; 25(13):1656-1676.
[20] Hess B, Kutzner C, van der Spoel D, Lindahl E. GROMACS 4: Algorithms for highly efficient, load-balanced, and scalable molecular simulation. *J Chem Theory Comput*. 2008; 4(3):435-447.
[21] Fiser A, Sali A. ModLoop: automated modeling of loops in protein structures. *Bioinformatics*. 2003; 19(18):2500-2501.
[22] Marti-Renom MA, Stuart AC, Fiser A, Sanchez R, Melo F, Sali A. Comparative protein structure modeling of genes and genomes. *Annu Rev Biophys Biomol Struct*. 2000; 29:291-325.
[23] The PyMOL Molecular Graphics System. In., Version 1.5.0.4 edn: Schrödinger, LLC.
[24] Gordon JC, Myers JB, Folta T, Shoja V, Heath LS, Onufriev A. H++: a server for estimating pK(a)s and adding missing hydrogens to macromolecules. *Nucleic Acids Res*. 2005; 33:W368-W371.
[25] Badieyan S, Bevan DR, Zhang CM. A salt-bridge controlled by ligand binding modulates the hydrolysis reaction in a family 5 endoglucanase. *Protein Eng Des Sel*. 2012; 25(5):223-233.
[26] Harris R, Olson AJ, Goodsell DS. Automated prediction of ligand-binding sites in proteins. *Proteins*. 2008; 70(4):1506-1517.
[27] Lipinski CA. Drug-like properties and the causes of poor solubility and poor permeability. *J Pharmacol Toxicol Methods*. 2000; 44(1):235-249.
[28] Lipinski CA, Lombardo F, Dominy BW, Feeney PJ. Experimental and computational approaches to estimate solubility and permeability in drug discovery and development settings. *Adv Drug Deliv Rev*. 2001; 46(1-3):3-26.
[29] Irwin JJ, Sterling T, Mysinger MM, Bolstad ES, Coleman RG. ZINC: A Free Tool to Discover Chemistry for Biology. *J Chem Inf Model*. 2012; 52(7):1757-1768.
[30] Olucha J, Meneely KM, Chilton AS, Lamb AL. Two structures of an N-hydroxylating flavoprotein monooxygenase: ornithine hydroxylase from Pseudomonas aeruginosa. *J Biol Chem*. 2011; 286(36):31789-31798.
[31] Packer M, Carver JR, Rodeheffer RJ, Ivanhoe RJ, DiBianco R, Zeldis SM, Hendrix GH, Bommer WJ, Elkayam U, Kukin ML *et al*. Effect of oral milrinone on mortality in severe chronic heart failure. The PROMISE Study Research Group. *N Engl J Med*. 1991; 325(21):1468-1475.
[32] Kobierska-Szeliga M, Czeczot H. Characterization of the genotoxic properties of nitrofurans: nitrofurazone and furazolidone. *Acta Biochim Pol*. 1994; 41(1):1-5.
[33] Gathocleous D, Shaw G. Purines, pyrimidines and imidazoles. Part 66. New syntheses of some uridine and N-alkoxycarbonyl-5-carboxamides, N-carbamoyl 5-carboxamides and 5-carboxamides J Chem Soc Perkin Trans 1. 1991. 2317-2321.

Microbial pathogens and strategies for combating them: science, technology and education (A. Méndez-Vilas, Ed.)

Integrative Conjugative Elements (ICEs) of the SXT/R391 group as vehicles for acquisition of resistance determinants, stable maintenance and transfer to a wide range of enterobacterial pathogens

P. Armshaw[1] and J. T. Pembroke[1]

[1] Laboratory of Molecular and Structural Biochemistry, Department of Chemical and Environmental Sciences and MSSI, Lonsdale Building, University of Limerick, Limerick, IRELAND. Email: tony.pembroke@ul.ie, Tel.: 353 61 202491; fax: 353 61 202568

Integrative conjugative elements (ICEs) belonging to the SXT/R391 group of mobile drug resistance elements are predominantly found in enterobacterial pathogens of human and waterborne origin. A key feature of such elements is their ability to stably integrate into their host *prfC* gene, initially truncating the gene but restoring *prfC* function by generating a novel hybrid *prfC* gene upon integration [1, 2]. Such stable integration into the genome of host organisms has consequences for the maintenance and spread of encoded antibiotic resistance determinants. We have surveyed the nature of *prfC* genes containing the unique SXT/R391 group 17bp integration site and demonstrate the breadth of possible ICE hosts amongst the enterobacteria. Many ICEs encode a range of antibiotic resistance determinants which appear to become associated with particular genomes through transposition or targeted integration into specific ICE hotspots [3, 4]. We have analysed the nature of these antibiotic resistance determinants amongst sequenced ICEs and have observed specific patterns of resistance and resistance determinant location. Interestingly, many ICE elements encode *rumAB* genes, which encode a mutagenic polymerase, polV that appears to be a targeted hotspot for insertion of many resistance determinants [5, 6]. A rational for insertion into such hotspots is discussed.

Keywords: SXT/R391-like elements; hotspots; mobile multi-drug resistance

1. Introduction

1.1. SXT/R391 family of Integrative Conjugative Elements

Mobile genetic elements play an important role in the generation of diversity and the dissemination of advantageous traits across bacterial populations, increasing individual strain fitness as they spread. Classical well-characterised families of mobile elements include plasmids and bacteriophage. Integrative Conjugative Elements or ICEs are a more recently characterised class which encode functions similar to those of plasmid, phage and transposons on the same element. ICEs are related to transposons as they site specifically integrate into their host genome, are similar to plasmids as they are capable of stimulating their own transfer between bacterial hosts by conjugation and have characteristics of bacteriophage as they encode phage-like regulatory genes. ICEs are therefore defined as mobile elements capable of mediating their own integration, excision and transfer by self-circularisation and conjugation between bacterial hosts [7]. Over 460 ICEs have been identified to date, (list available at the ICEberg database [8]), in a variety of Gram positive and Gram negative bacterial genomes with this number likely to increase significantly with whole genome sequencing. Therefore, ICEs are sub-grouped into families based on integrase similarity and the specific integration site they utilise. The largest known family of ICEs is the SXT/R391 group, currently consisting of 89 ICEs [9].

The SXT/R391 family ($ICE_{SXT/R391}$) are found in Gram negative hosts and integrate into the *prfC* gene without disrupting gene function [1]. They encode several antibiotic and heavy metal resistance determinants and mutagenic DNA repair genes and promote the mobilisation of non-transmissible genomic islands and virulence plasmids between hosts [5, 10]. Sequencing of ICE R391 and ICE SXT revealed that both ICEs shared a core molecular backbone [5, 11, 12] of genes related to basic ICE functionality (integration, excision and conjugative transfer). Subsequent members were allocated to the $ICE_{SXT/R391}$ family based on this conserved backbone and synteny. To be categorised as an SXT/R391 family member, an ICE must encode an integrase gene highly similar to *int*SXT/R391 and integrate only into the *prfC* gene [13].

The core $ICE_{SXT/R391}$ backbone of genes contributes to the ICEs' ability to be stably maintained within and transferred between a range of enterobacterial hosts. Comparative analysis has allowed determination of the locations of accessory gene insertion into the core $ICE_{SXT/R391}$ genome and allowed observation of the diversity of encoded antibiotic and other resistance determinants.